

Article

Heterogeneous Phases Reaction Equilibrium in an Oxy-Thermal Carbide Furnace

Wenjie Xiong^{1,2,†}, Xiaohui Chen^{2,3,*}, Quanyong Wang^{1,2}, Min Gao¹, Danxing Zheng^{2,†}, Yuliang Mai¹ and Wei Hu^{1,*}

¹ Guangdong Research Institute of Petrochemical and Fine Chemical Engineering, Guangzhou 510665, China; wenjie_xiong@yeah.net (W.X.); wagnqy89@163.com (Q.W.); happysue2001@163.com (M.G.); maiyul@163.com (Y.M.)

² College of Chemical Engineering, Beijing University of Chemical Technology, Beijing 100029, China; dxzh@mail.buct.edu.cn

³ Energy and Environment Research Center, Shenzhen Institute of Standards and Technology, Shenzhen 518031, China

* Correspondence: xiaohui4187@sina.com (X.C.); gracehz@126.com (W.H.); Tel.: +86-020-32373090 (W.H.)

† These authors contributed to this work equally.

Received: 29 October 2019; Accepted: 2 January 2020; Published: 3 January 2020



Abstract: This work focuses on revealing the chemical reaction equilibrium behaviors of gas–liquid–solid heterogeneous phases in an oxy-thermal carbide furnace. From a CaC₂ formation mechanism investigation, it was determined that a one-step mechanism occurs when there is an excess of C and a high CO partial pressure, which inhibits the formation of Ca in the system, and a two-step mechanism occurs when there is insufficient C and a low CO partial pressure, which promotes the formation of Ca. Based on the calculated results of the equilibrium compositions at 100 kPa and different temperature conditions, the chemical reaction equilibrium behaviors of gas–liquid–solid heterogeneous phases in an oxy-thermal carbide furnace were analyzed at conditions of excess C and insufficient C.

Keywords: oxy-thermal carbide furnace; reaction equilibria; heterogeneous phases; calcium carbide

1. Introduction

Calcium carbide (CaC₂) is an important chemical produced from the reaction of CaO with coke in a carbide furnace. It is mainly used to produce acetylene and other derivatives, such as polyethylene and polyvinyl chloride [1]. In 2012, the production of CaC₂ was more than 18 million tons [2]. At present, the reaction of CaO with coke to produce CaC₂ is mainly achieved in a moving-bed reactor with electric arc heating. Inside the reactor, the temperature is above 2200 K, and the mixture of CaO and coke reacts to produce CaC₂. However, the energy consumption is extremely large (e.g., up to 3000 kWh/t), and the purity of CaC₂ obtained is only 81.8% (wt.) [3]. Thus, many researchers have studied an alternative energy-saving process, the oxygen thermal process [4,5].

Two opposing views regarding the CaC₂ formation mechanism have been debated for many years, namely, a one-step mechanism and a two-step mechanism. The one-step mechanism indicates that CaO reacts with C directly to form CaC₂ as per Equation (1), whereas, in the two-step mechanism, CaO reacts with C to produce Ca, which then reacts with C to form CaC₂ according to Equations (2) and (3). The difference between the two views is whether Ca gas is produced during CaC₂ formation:





Tagawa and Sugawara [6], Millur [7], and EI-Naas [8,9] suggested the two-step CaC_2 formation mechanism in 1962, 1968, and 1998, respectively. They found that the initial reaction temperature of CaO with C is 1873–2073 K, and the CO partial pressure is 6.7–26.7 kPa. Rai detected the existence of Ca during the reaction of CaO with C under high vacuum at 1500 K, at which point CaC_2 was produced; thus, he concluded that the CaC_2 formation mechanism is a two-step process [10]. In 1975, Brookes [11] reported that the CaC_2 formation has a close relationship with the temperature and CO partial pressure. He discovered that, when the CO partial pressure is 6.7 kPa, the initial reaction temperature of CaO with C is 1923–2023 K. In 1983, Wiik [12] confirmed the two-step mechanism by an experiment of Ca reacting with C to produce CaC_2 . However, many other researchers believe that the one-step mechanism is a more likely scenario. In 1979, 1987, and 2001, Kim [13] and Wang [14] reported that the CaC_2 formation mechanism is a one-step process. They found that, when the CO partial pressure is 100 kPa, the initial reaction temperature of CaO with C is 1850–2043 K, and no smelt is observed in the reaction residue, which is in accordance with the research of Thoburn [15] in 1965. Recently, Li [16] argued in favor of a two-step mechanism after performing extensive research on CaC_2 formation. Muftah [17] also performed research on the CaC_2 formation mechanism in 1996, but he failed to find proof of which mechanism is followed. Later, when conducting research on an oxy-thermal carbide furnace, Guo [18] directly treated the reaction as following a two-step mechanism.

Stals [19] measured and calculated the three-phase equilibrium in sulfur dioxide + p-toluidine binary. However, the CaC_2 - CaO liquid–solid phase heterogeneous reaction equilibrium system has not been studied extensively, mainly because the eutectic temperature of the CaC_2 - CaO binary system is extremely high and the melt cannot be easily observed. In 1923, Ruff and Foerster [20] reported that the eutectic temperature of the CaC_2 - CaO binary system is 1910 K, and the mole fraction of CaC_2 is 0.62. Flusin and Aall [21] found that CaC_2 and CaO could form a eutectic of CaC_2 - CaO at 2253 K. In this system, there are two eutectic points. One of them is at 2023 K when the mole fraction of CaC_2 is 0.68, and the other is at 2073 K when the mole fraction of CaC_2 is 0.356. Li [22] measured the reaction activation energy of R2 by the so-conversional method and found that it was 213 kJ/mol when the temperature is higher than 1971 K but 477 kJ/mol when the temperature is below 1971 K. He attributed this relatively large difference to a predicted eutectic point of the CaC_2 - CaO mixture at 1971 K. Kameyama [23] introduced the production of CaC_2 from CaO and C and he proposed that, above 1200 K, the interdiffusion between CaO and C occurs to form the solid CaO-C and CaC_2 gradually and that CaC_2 and CaO could form four eutectics of CaC_2 - CaO between 2100–2200 K. Juzza and Schuster [24] measured the liquid temperature of a $\text{CaC}_2 + \text{CaO}$ mixture system using optical pyrometry in 1961. They used CaC_2 synthesized from metallic Ca and C in a Fe crucible. The reported impurities in the CaC_2 were small amounts of CaO . The samples were not in contact with graphite during the experiments but were instead placed on titanium carbide to reduce the interaction of carbon with the sample. The time of the heating of the samples and the observation of the melting temperature were limited to reduce the possible evaporation of the sample. The reported phase diagram is for a simple eutectic binary system with a eutectic point at a CaC_2 mole fraction of 0.48 and 2103 K. The results from all studies are summarized in Figure 1. Muller [7] argued that the work of Juzza and Schuster is the most reliable of all of the studies cited, and, thus, most researchers used the data of Juzza and Schuster in subsequent studies.

In the CaC_2 manufacturing process, coke (88% C) and lime (92% CaO) entering from the top of the oxy-thermal carbide furnace react with oxygen entering from the bottom. A part of the coke combusts to release heat, driving the furnace temperature above 2200 K, and the CaO reacts with another part of the coke to produce CaC_2 . Based on the work of Muftah [17], Guo [18] showed that the reaction in the oxy-thermal carbide furnace is a gas–solid reaction system, and thus the system can be simplified as a C-O-Ca reaction system after the impacts of impurities, such as iron oxide, aluminum oxide, and silicon oxide, on the reactions in the furnace are ignored. Guo concluded that the CaC_2 formation temperature is 1755 K, and he proposed a four-stage reaction process with the increase of temperature

in the furnace: a combustion stage, the formation stage of CaC_2 , the equilibrium stage of CaC_2 , and a decomposition stage. The results indicate that, during the combustion stage, adding an appropriate amount of C is favorable for CO_2 formation, as it improves the reaction heat supply ability of the exothermic combustion reaction and decreases feed consumption. During the formation stage of CaC_2 , the appropriate parameters of C addition, temperature, and pressure are 10.7 mol, 2473.15 K, and 100 kPa, respectively. However, he ignored the liquid phase in the furnace.

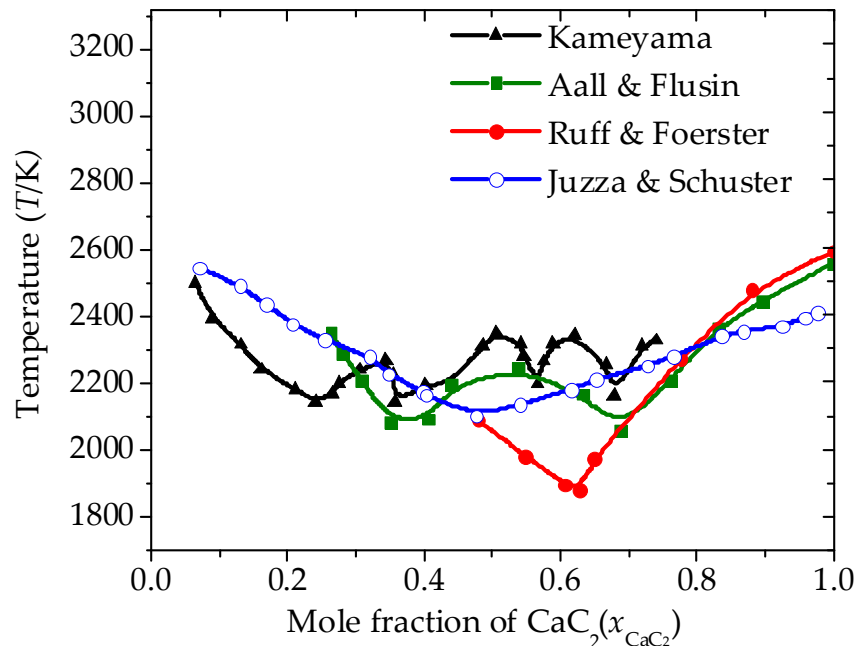


Figure 1. Phase diagram of the CaC_2 -CaO binary system.

Ji [25] studied the CaC_2 formation mechanism focusing on R2 and R3. He supposed that the different reaction mechanisms reported in the literature result from the differences in reaction pressure and temperature, and thus they do not contradict each other. At temperatures higher than 1573 K, CaC_2 forms directly from CaO and coke. The result shows that the initial C/CaO ratio influences the reaction mechanism. An initial C/CaO ratio of less than three results in a three-stage mechanism, whereas an initial C/CaO ratio greater than three results in a two-stage mechanism. The suggested optimum conditions are approximately 253.3 kPa at 2200–2273 K and 405.3 kPa or higher at 2373 K.

This work aims to reveal the chemical reaction equilibrium behaviors of gas–liquid–solid heterogeneous phases in an oxy-thermal carbide furnace. To this end, the CaC_2 formation mechanism was studied. In addition, the chemical reaction equilibrium behaviors of the gas–liquid–solid heterogeneous phases were analyzed at conditions of excess C and limited C.

2. Basic Thermodynamic Behavior of the Chemical Reaction System

Li [26] reported that magnesium oxide, iron oxide, and other minerals, such as calcium fluoride, in the furnace have only a slight influence on the CaC_2 formation, and the minimal silicon oxide and aluminum oxide can only favor the pathway of R2 to produce CaC_2 . Thus, the reaction system can be simplified as the reaction system described in Guo's work [18].

In the oxy-thermal carbide furnace at different temperature and pressure conditions, different reactions exist among O_2 , C, and CaO. In addition to R1, R2, and R3 shown as Equations (1)–(3), respectively, there are two other reactions, R4 and R5, which are shown in Equations (4) and (5), respectively. However, the reactions are not independent, and they tend not to exist simultaneously under a single set of temperature and pressure conditions:



The phase diagram of the CaC₂-CaO binary system is drawn in Figure 2 based on the data measured by Juza and Schuster. Then, Equations (6) and (7) were obtained using the solid-liquid two-phase equilibrium basic model [27] to regress the experimental data:

$$T_1 = \frac{-7627.57}{\ln(1 - x_{CaC_2}) - 2.94}, \quad (6)$$

$$T_2 = \frac{-11,923.50}{\ln x_{CaC_2} - 4.93}, \quad (7)$$

$x_{CaC_2} = 0.49$ when $T_1 = T_2 = 2103.4$ K.

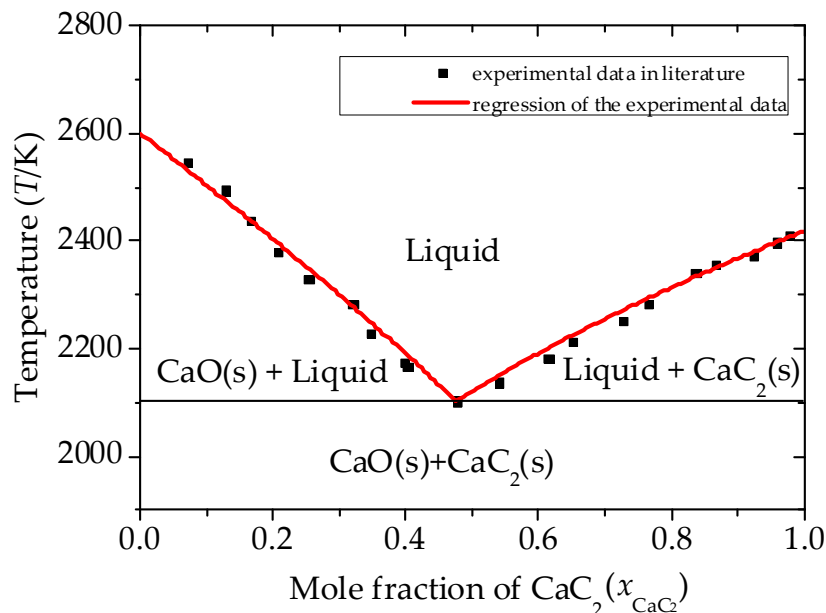


Figure 2. Experimental data fitting of phase diagram of CaC₂-CaO binary system (Liquid contains CaO (l) and CaC₂ (l)).

The liquid region is a mixture of CaC₂ (L) and CaO (L), the liquid + CaO (s) region is a mixture of CaC₂ (L), CaO (L), and CaO (s), and the liquid + CaC₂ (s) region is a mixture of CaC₂ (L), CaO (L) and CaC₂ (s).

2.1. *pVT Behavior of the Gas Phase*

Assuming that the Peng–Robinson [28] Equations (8)–(11) can describe the *pVT* behavior of the gas phase in the oxy-thermal carbide furnace, the relationship of fugacity coefficient change with the temperature and pressure of Ca, CO and O₂ are shown as Figures 3–5, as calculated by Aspen plus technology software [29]:

$$p = \frac{RT}{V-b} - \frac{a(T, \omega)}{V(V+b)}, \quad (8)$$

$$b = 0.07779 \frac{RT_c}{p_c}, \quad (9)$$

$$\alpha(T, \omega) = \left[1 + \left(0.37464 + 1.54226\omega - 0.26992\omega^2 \right) \left(1 - T_r^{\frac{1}{2}} \right) \right]^2, \quad (10)$$

$$T_r = \frac{T}{T_c}, \quad (11)$$

where the term (p, T, V) represents the specified state at pressure, temperature, and volume, respectively. The term (p_c, T_c, ω, R) stands for the specified state at critical pressure, critical temperature, acentric factor, and thermodynamic constant, respectively, which could be obtained from the literature [30] for each substance.

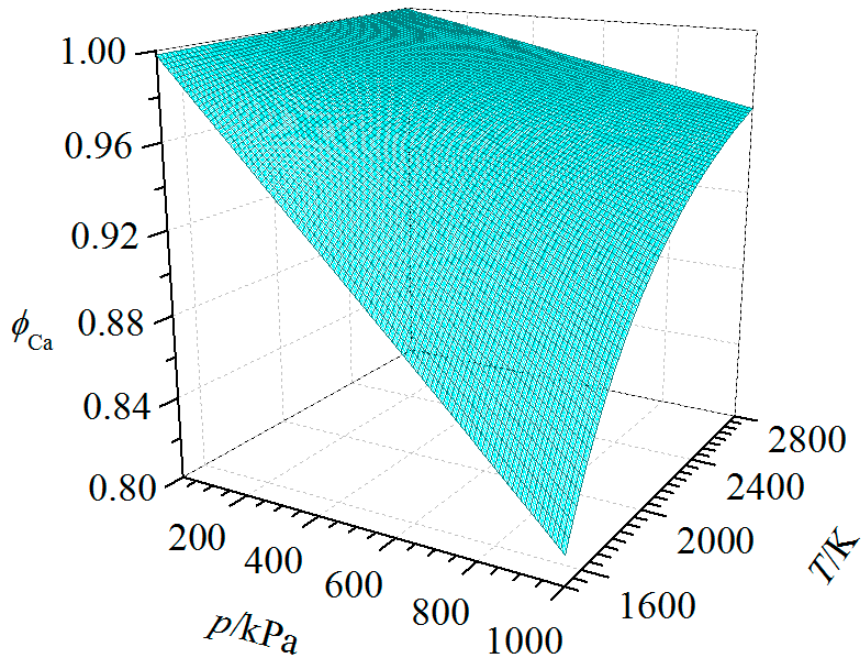


Figure 3. Fugacity coefficient of Ca.

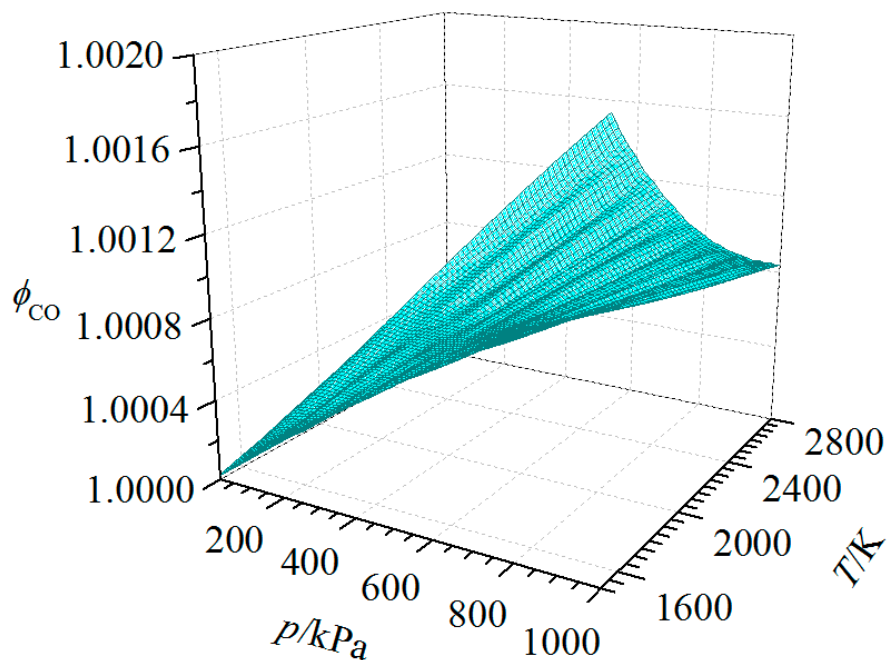


Figure 4. Fugacity coefficient of CO.

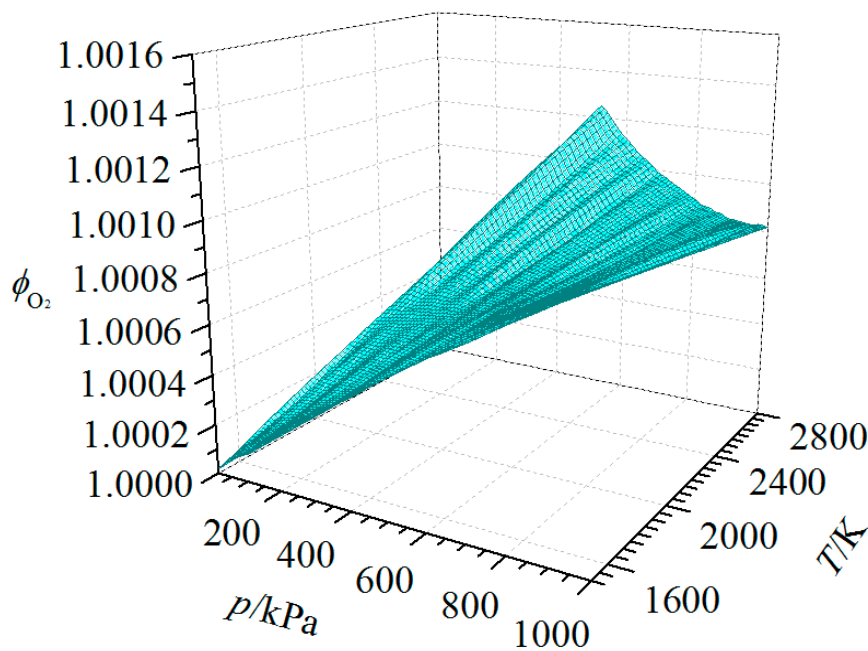


Figure 5. Fugacity coefficient of O₂.

Figure 3 is clearly different from Figures 4 and 5. In the range of 1500–2800 K and 10–1000 kPa, ϕ_i of Ca is below 1 and decreases with increasing temperature and decreasing pressure, whereas ϕ_i of CO and O₂ are above 1, and they increase with increasing temperature and decreasing pressure. ϕ_i of Ca deviates further from 1 than ϕ_i of CO and O₂, which means that temperature and pressure have greater effects on the non-ideal behavior of Ca than on CO and O₂.

Summarizing Figures 3–5, the properties of CO and O₂ approach those of an ideal gas because ϕ_i of CO and O₂ do not deviate far from 1, whereas Ca cannot be treated as an ideal gas because ϕ_i of Ca deviates significantly from 1. Thus, the Peng–Robinson equation can be adopted to describe the gas properties of each gas in the furnace instead of the ideal gas equation.

2.2. Thermodynamic Equilibrium of the Reaction System

In the oxy-thermal carbide furnace, because there are small amounts of CaO, CaC₂, and C in the gas phase and small amounts of CO, Ca, and O₂ in the liquid phase, they can be ignored. Thus, the ratio between the gas phase and liquid phase is assumed to be mainly determined by the chemical reaction equilibrium. The partial pressure of O₂ in the system is set at 100 kPa based on the industrial data since O₂ is inputted into the system to react with C to provide heat and energy in the industrial production of CaC₂. The mass of CO₂ accounts for 0.98% of the off-gas in the industrial production process of CaC₂, and the percentage of CO is above 90% [4,18], which demonstrates the slight formation of CO₂ in the system. Thus, the influence of CO₂ can be ignored in this work.

In the oxy-thermal carbide furnace, the occurrence of each reaction depends on the temperature and pressure. The thermodynamic property data of the substances in the furnace are listed in Table 1, which are compiled from several references [31–33] after evaluation in Guo's work [18] and Li's work [22].

Table 1. Thermodynamic data $H_{i,298.15\text{ K}}^\theta$, $S_{i,298.15\text{ K}}^\theta$ and $C_{p,i}$ of the components in the furnace.

Substance	T	$H_{i,298.15\text{ K}}^\theta$	$S_{i,298.15\text{ K}}^\theta$	$C_{p,i}$
	K	J·mol ⁻¹	J·mol ⁻¹ ·K ⁻¹	J·mol ⁻¹ ·K ⁻¹
C (graphite)	298.15–1100 1100–4073	0	5.74	$0.084 + 0.038911 \times T - 146,400 \times T^{-2} - 0.000017364 \times T^2$ $24.435 + 0.000418 \times T - 3,163,100 \times T^{-2}$
O ₂ (g)	298.15–3000	0	205.04	$29.957 + 0.00418 \times T - 167,400 \times T^{-2}$
CO (g)	298.15–2800	-110,541	197.527	$28.409 + 0.0041 \times T - 46,000 \times T^{-2}$
Ca (g)	298.15–2800	-178,146	154.674	20.832
CaO (s)	298.15–2845	-635,090	37.75	$58.7912 - 1,147,146 \times T^{-2} - 133.904 \times T^{-0.5} + 102,978,787.9 \times T^{-3}$
CaO (l)	298.15–2845	-555,594	65.69	$58.7912 - 1,147,146 \times T^{-2} - 133.904 \times T^{-0.5} + 102,978,787.9 \times T^{-3}$
CaC ₂ (s)	298.15–1275 1275–3000	-53,030.3	79.1553	$64.4336 + 0.008368 \times T$ 75.1028
CaC ₂ (l)	298.15–3000	3802.2	96.825	75.1028

For each component i in the furnace, entropy, enthalpy and Gibbs energy could be obtained by Equations (12)–(15):

$$S_i^\theta(T) = S_{i,298.15\text{ K}}^\theta + \int_{298.15}^T \frac{C_{p,i}}{T} dT, \quad (12)$$

$$H_i^\theta(T) = H_{i,298.15\text{ K}}^\theta + \int_{298.15}^T C_{p,i} dT, \quad (13)$$

$$G_i^\theta(T) = H_i^\theta(T) + TS_i^\theta(T). \quad (14)$$

In addition, for each possible reaction j in the furnace, reaction Gibbs energy could be calculated by Equation (15):

$$\Delta G_j(T, p) = \sum_i v_{j,i} G_{j,i}^\theta(T) + RT \ln \prod_i \left(\frac{\varnothing_i y_i p}{p^\theta} \right)^{v_{j,i}}, \quad (15)$$

where $v_{j,i}$ is stoichiometric coefficient of component i in reaction j , and y_i is the mole fraction of component i in the gas phase.

According to the thermodynamic property data and the equation models above, ΔG_j - T - p plots are shown in the following figures.

The figures above express the relationship of each reaction $\Delta G_j(T, p)$ with T and p_{CO} in the furnace. The curved surfaces are the behavior surfaces of $\Delta G_j(T, p)$, which is the surface corresponding to the Gibbs energy of the reaction j at a given temperature and pressure, and colored areas on the T - p_{CO} coordinate are the shadow of $\Delta G_j(T, p) \leq 0$. The lines on the T - p_{CO} coordinate are the shadows of $\Delta G_j(T, p) = 0$, which indicate that the equilibrium of the reaction starts to shift towards the formation of products, creating the reaction products. The irregular inflections to form bulges on the behavior surfaces are caused by the eutectic of CaC₂ and CaO mixture above the temperature of 2103.4 K.

Figure 6 shows the relationship of the $\Delta G_1(T, p)$ behavior surface of R1 with T and p_{CO} . When $\Delta G_1(T, p) = 0$, the shadow on the T - p_{CO} coordinate is a boundary line of the shadow part. The boundary line indicates that $\Delta G_1(T, p) = 0$ and that the required temperature of R1 gradually drops as p_{CO} decreases within the range of 1500–2800 K and 10–1000 kPa. When p_{CO} is 10 kPa, the temperature of $\Delta G_1(T, p) = 0$ is at a minimum value of 1950.0 K.

Figure 7 shows the relationship of the $\Delta G_2(T, p)$ behavior surface of R2 with T and p_{CO} . The curve lines on the T - p_{CO} coordinate are the shadows of $\Delta G_2(T, p) = 0$ at different p_{Ca} values, which means that the equilibrium of the reaction shifts to the formation of products. When $\Delta G_2(T, p) = 0$, the temperature at which the equilibrium of R2 shifts towards the formation of products decreases as p_{CO} and p_{Ca} decrease. When p_{CO} and p_{Ca} are 10 kPa, the temperature of $\Delta G_2(T, p) = 0$ is at its lowest value of 2100.0 K.

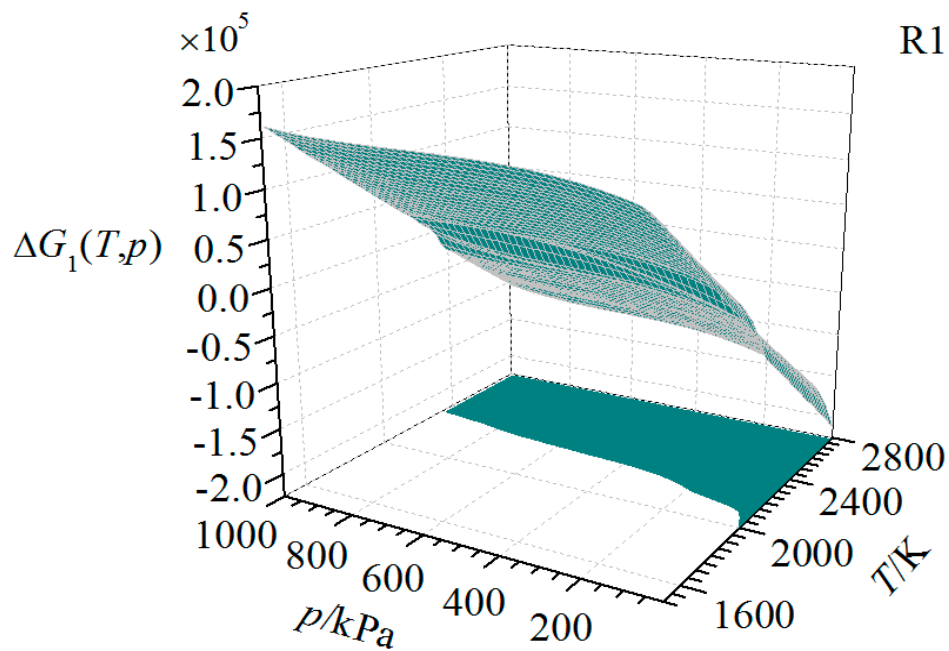


Figure 6. Gibbs energy dependence on temperature and CO partial pressure for reaction R1.

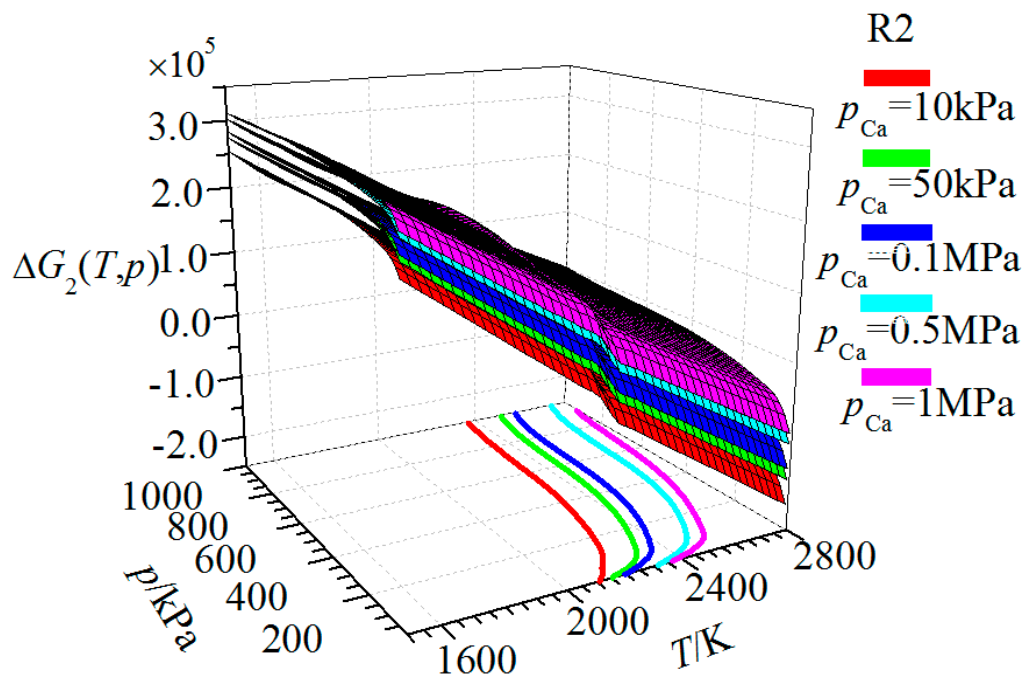


Figure 7. Gibbs energy dependence on temperature and Ca and CO partial pressure for reaction R2.

Figure 8 shows the relationship of the $\Delta G_3(T,p)$ behavior surface of R3 with T and p_{Ca} . The $\Delta G_3(T,p)$ of R3 is always below 0 in the range of 1500–2800 K and 10–1000 kPa. Thus, before reaching equilibrium, R3 shifts towards the formation of products, i.e., as long as Ca and C are present, they will react to produce CaC_2 . In other words, the reverse reaction of R3 will only shift towards the formation of initial substances. This is in opposition to previous reports in the literature [18,25]. According to the analysis above, in the condition range of 1500–2800 K and 10–1000 kPa, Ca can easily react with C to produce CaC_2 , but CaC_2 can hardly decompose.

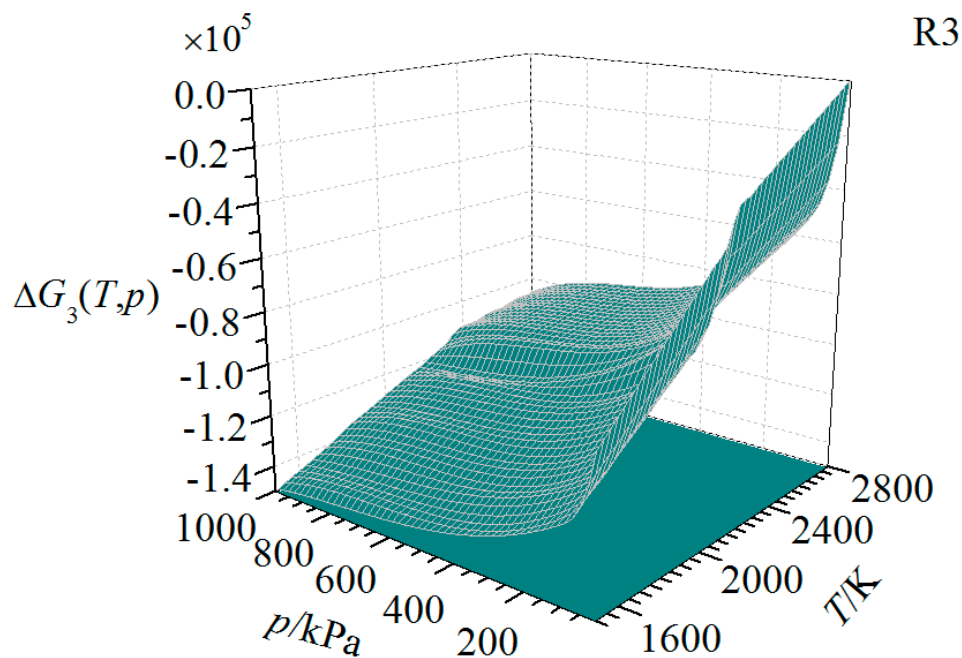


Figure 8. Gibbs energy dependence on temperature and Ca pressure for reaction R3.

Figure 9 shows the relationship of the $\Delta G_4(T,p)$ behavior surface of R4 with T and p_{CO} . It indicates that the $\Delta G_4(T,p)$ of R4 is always below 0; thus, in the condition range of 1500–2800 K and 0–1000 kPa, before reaching equilibrium, R4 shifts towards the formation of the products, i.e., C reacts with O_2 to produce CO.

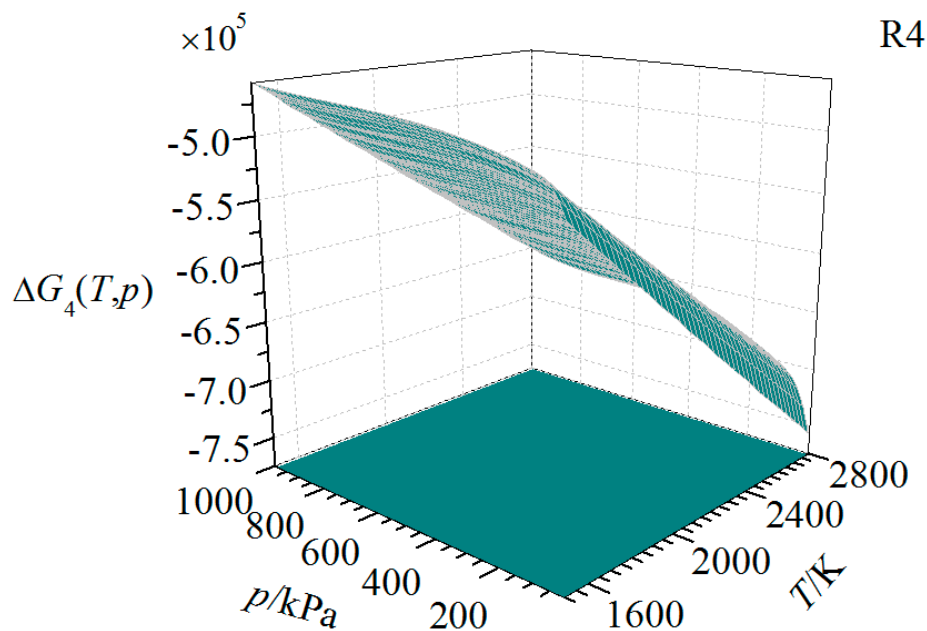


Figure 9. Gibbs energy dependence on temperature and CO partial pressure for reaction R4.

Figure 10 shows the relationship of the $\Delta G_5(T,p)$ behavior surface of R5 with T and p_{CO} . The curved lines on the T - p_{CO} coordinates are the shadows of $\Delta G_5(T,p) = 0$, which means that the reaction starts to shift to the formation of products. When $\Delta G_5(T,p) = 0$, the temperature at which the equilibrium of R5 shifts towards the formation of products decreases as p_{CO} and p_{Ca} decrease. When p_{CO} and p_{Ca} are 10 kPa, the temperature of $\Delta G_5(T,p) = 0$ is at its lowest value of 2150.0 K.

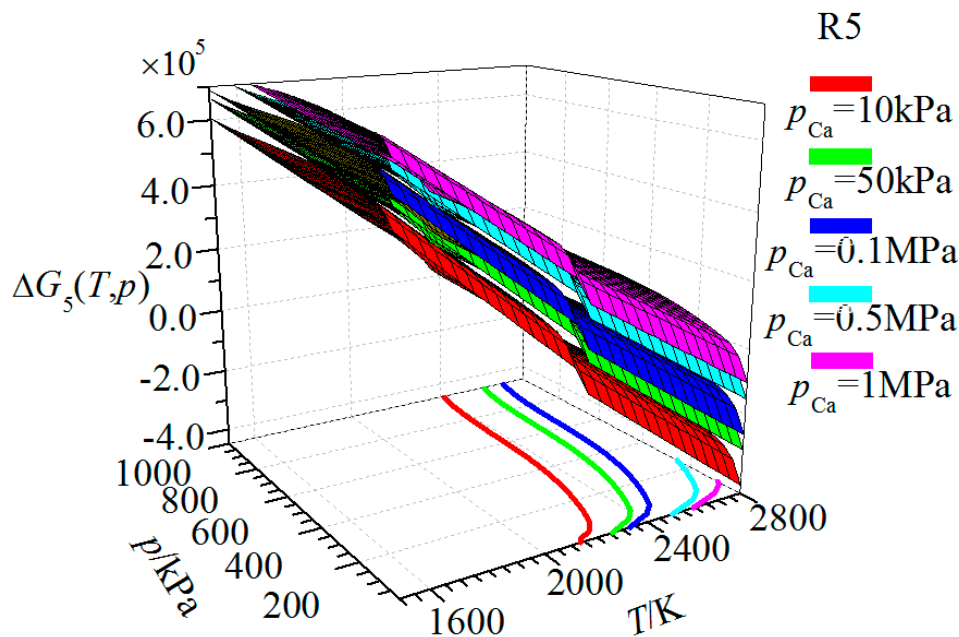


Figure 10. Gibbs energy dependence on temperature and Ca and CO partial pressure for reaction R5.

Integrating R2, R3, and R5 shows that both R2 and R5 could create Ca at some T and p_{CO} , but whether Ca presents in the system as the equilibrium approaches depends on R3. According to the analysis above, as long as C and Ca are present in the reaction system, the equilibrium of R3 will shift to the formation of CaC_2 . However, the amount of C is determined by the initial composition of the system, so, if there is an excess of C, the Ca from R2 and R5 will react with C and form CaC_2 at any values of T and p_{CO} before reaching equilibrium. Therefore, when reaching equilibrium, Ca does not exist in the system. Conversely, if the initial amount of C is insufficient, C will be consumed by R2 and R5 when approaching equilibrium and Ca will be present in the system.

In summary, whether Ca presents in the equilibrium system or not depends on T , p_{CO} , and the initial quantity C.

In the practical manufacture of CaC_2 , the operating pressure in the oxy-thermal carbide furnace is typically approximately 101.3 kPa. Taking 101.3 kPa as the pressure condition in the following discussion, when $\Delta G_j(T,p) = 0$, the equilibrium of reaction j starts to shift to the formation of products. C initially reacts with O_2 according to R4 to release heat, and the furnace is heated. As the temperature increases in the furnace, the first reaction to occur is R1, and, at this point, the temperature is 2090.0 K and CaC_2 is produced in the furnace. When the temperature reaches 2360 K, R2 begins to produce Ca and CO, but the Ca will react with C to form CaC_2 through R3. When the temperature increases to 2490.0 K, R5 occurs, and the CaC_2 will decompose to produce Ca and CO with the participation of the CaO.

3. Equilibrium Composition in the Oxy-Thermal Carbide Furnace

Considering a system with multiple components and heterogeneous phases at constant temperature and pressure, there are chemical reactions and mass transfer among the phases before the system reaches equilibrium. At this point, the state change in the system is irreversible, which tends to make the system reach equilibrium. If G^t is expressed as the function of the amount of each component in the heterogeneous phases under the mass conservation law, there is an amount of each component that can minimize G^t , and this is the effective method to solve problems in a system of multiple components and heterogeneous phases, such as in an oxy-thermal carbide furnace. Ignoring the influence of minerals, such as iron oxide, aluminum oxide, and silicon oxide, Equations (16)–(18) can be applied to the oxy-thermal carbide furnace according to Gibbs energy theory [34,35]:

$$G_{\min}^t = \sum n_i^g G_i(T) + \sum n_i^g RT \ln \frac{y_i \phi_i p_i}{p^\theta} + \sum n_i^l G_i(T) + \sum n_i^l RT \ln x_i + \sum n_i^s G_i(T), \quad (16)$$

$$y_i = \frac{n_i^g}{\sum n_i^g}, \quad (17)$$

$$x_i = \frac{n_i^l}{\sum n_i^l}. \quad (18)$$

Considering a reaction system composed of M elements and N components, A_m is the number of the m th atom and B_i the molar quantity of the i th component. a_{im} is the number of the m th atom of the i th component, which is the atomic coefficient. There is

$$A_m = \sum_i a_{i,m} B_i \quad (i = 1, 2, \dots, N, m = 1, 2, \dots, M). \quad (19)$$

In this work, it is assumed that there is chemical equilibrium in the oxy-thermal carbide furnace between the gas, liquid, and gas solid phases, whereas the gas-liquid and gas-solid phase equilibrium and adsorption can be ignored. In addition, when the liquid and solid phases reach equilibrium, Equation (20) can be obtained as follows:

$$\frac{n_{\text{CaC}_2}^l}{n_{\text{CaC}_2}^s} = \frac{x_{\text{CaC}_2}^s - x_{\text{CaC}_2}}{x_{\text{CaC}_2} - x_{\text{CaC}_2}^l}. \quad (20)$$

Figure 11 is the calculation flow diagram of equilibrium components of the system. In this diagram, the left region, right region and middle region represent the liquid + CaO (s) region, the liquid + CaC₂ (s) region, and the liquid region in Figure 2, respectively. EC stands for equilibrium components and LP means lever principle. G_{\min} is the minimum Gibbs energy of the system at each condition.

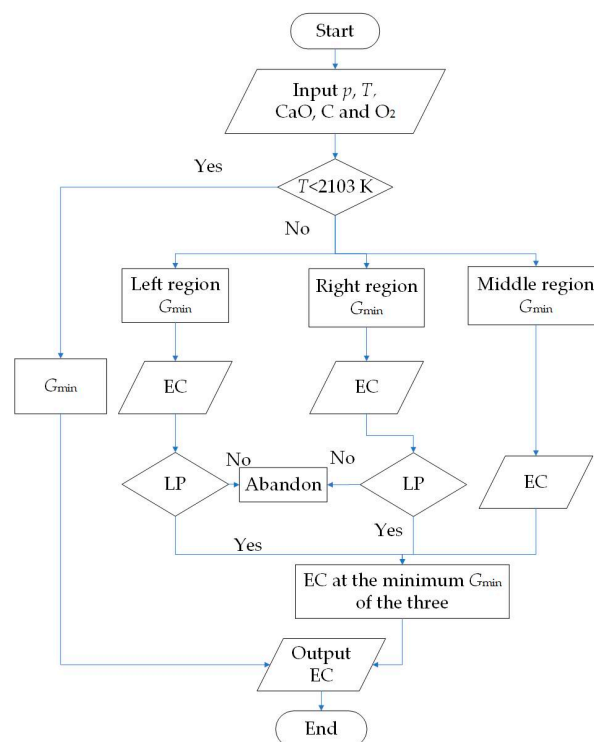


Figure 11. Calculation flow diagrams of the equilibrium components.

3.1. Analysis of the Equilibrium Composition under Conditions of Excess C

As discussed in Section 2, the amount of C present has an effect on the presence of Ca. When C is present in excess, the produced Ca can quickly react with C to form CaC_2 . Therefore, there is no Ca in the system when the system reaches equilibrium. In contrast, Ca will persist in the system when C is limited, so there is Ca when the system reaches equilibrium. Therefore, the amount of C in the system should be considered when studying the equilibrium composition. After energy coupling calculation, the appropriate initial amounts of CaO, O_2 and C are 1, 2.5 and 7.5 mol, respectively. Based on this theory, different equilibrium compositions are obtained under excessive C and limited C conditions.

At 100 kPa, 1 mol of CaO, 2.5 mol of O_2 , and 7.5 mol of C are added to the oxy-thermal carbide furnace. Figures 12–14 were obtained by the calculation of MathCAD software (version 15, Parametric Technology Corporation, Boston, MA, USA) based on the equations and theory above. Figure 12 presents the conversions of CaO and C at each reaction temperature. Figure 13 expresses the equilibrium composition with temperature. Figure 14 illustrates the equilibrium phase composition with temperature.

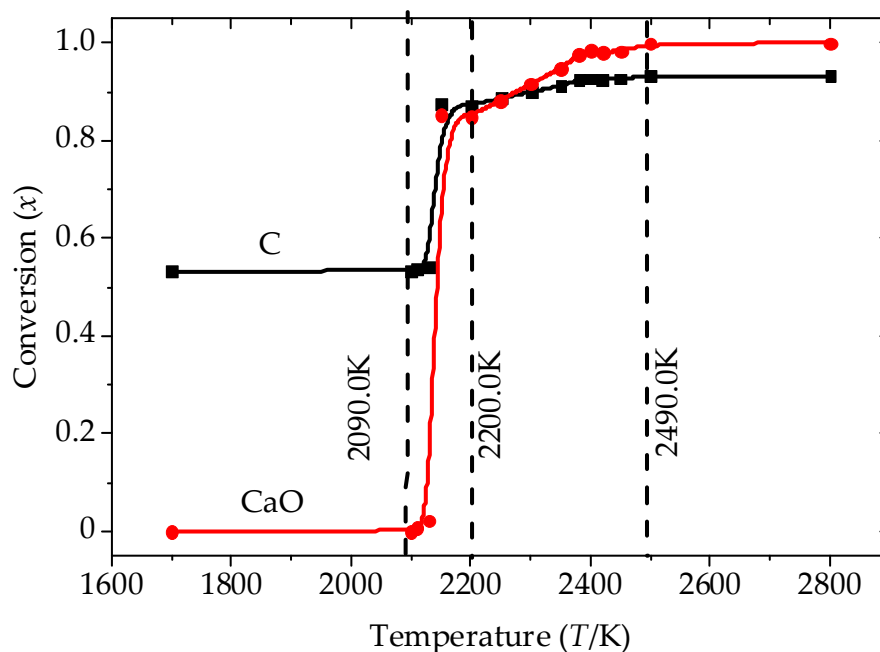


Figure 12. The conversion of C and CaO at each reaction temperature.

Figures 12 and 13 indicate that, in the temperature range of 1600–2800 K, O_2 is completely consumed to produce CO. At 2090 K, C and CaO reduce sharply to produce CaC_2 and CO, i.e., the conversions increase, which matches the discussion in Section 2. With the increase of temperature, CaO and C gradually decrease and the conversion increases to 100% and 99% and CaC_2 increases to 1 mol. In the temperature range of 1700–2800 K, the amount of Ca is zero throughout because of the excess C and the pressure not being conducive to the formation of Ca. This result is also consistent with the discussion in Section 2.

Figure 13 shows the chemical reaction equilibrium behavior of gas–liquid–solid heterogeneous phases in the condition of excess C in the oxy-thermal carbide furnace. At approximately 2100 K, CaC_2 is produced to form a eutectic with CaO, which matches the description in Figure 12. CaO (L) and CaC_2 (L) increase with increasing temperature. At approximately 2200 K, CaC_2 (L) reaches a peak and then gradually diminishes. This trend can be explained by Figure 12. When the reaction occurs, the amount of CaC_2 gradually increases, and the equilibrium composition state of CaC_2 in the system moves from the Liquid + CaO (s) region directly to the Liquid + CaC_2 (s) region. This leads to the decrease of CaC_2 and the conversion of CaO, appearing as the peak in Figure 14. Due to CaO (s)

rapidly disappearing after the reaction occurs at approximately 2200 K, CaC_2 (s) has a peak and then increases slowly, but, at approximately 2400 K, CaC_2 (s) decreases sharply because the mole fraction of CaC_2 is close to 1 and the temperature reaches the melting point of CaC_2 , which is 2400 K.

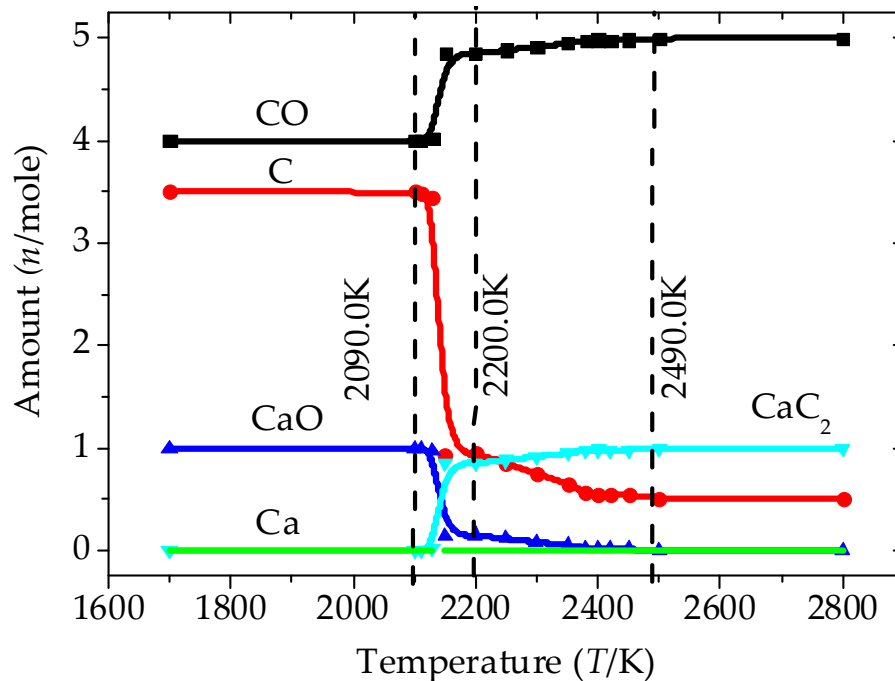


Figure 13. The equilibrium composition at each reaction temperature.

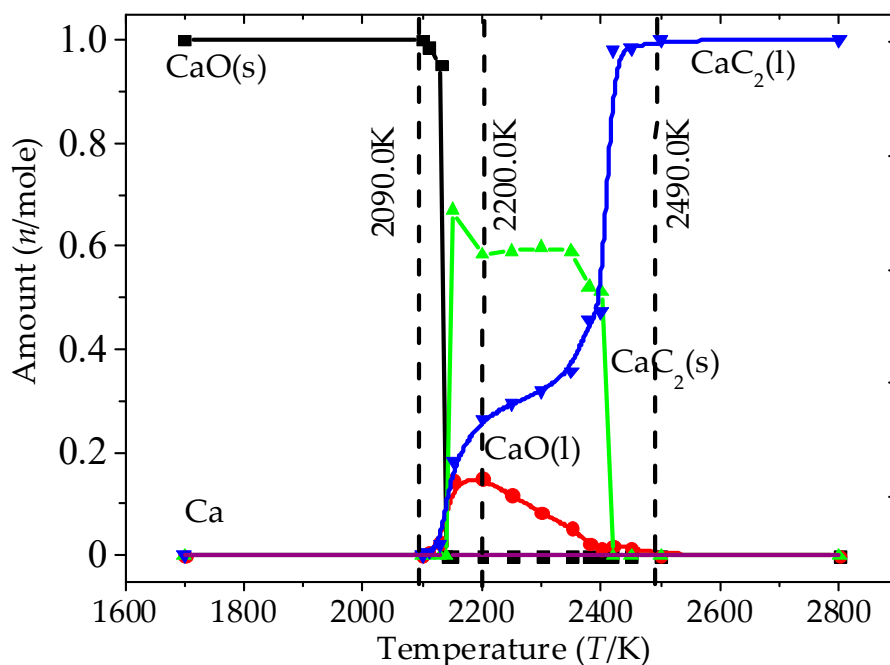


Figure 14. The equilibrium phase composition at each reaction temperature.

To validate the equilibrium components, confirmation of the calculation was made as shown in Figure 15. The system equilibrium components are illustrated at three different temperature conditions, which are 2130 K, 2200 K, and 2420 K. At 2130 K, the system point is in the liquid + CaO (s) region and x_{CaC_2} is 0.03. At 2200 K, the system point is in the liquid + CaC_2 (s) region with the x_{CaC_2} of 0.85.

However when the temperature reaches 2420 K, the system point is in the liquid region, and the x_{CaC_2} is 0.98.

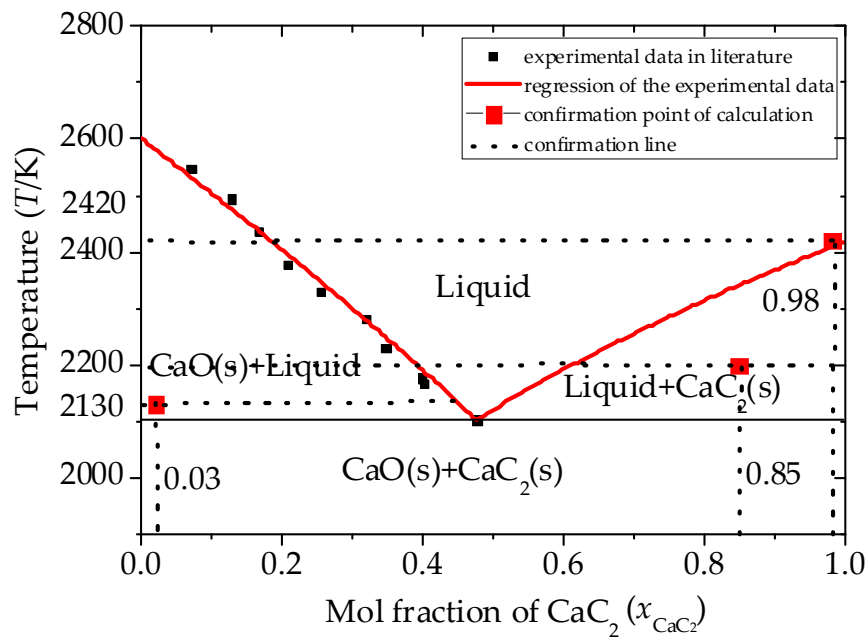


Figure 15. Confirmation of the calculation (Liquid contains CaO (L) and CaC_2 (L)).

3.2. Analysis of the Equilibrium Composition at a Condition of Limited C

Figures 16–18 were obtained under the conditions of a pressure of 100 kPa and a composition of 1 mol of CaO, 2.5 mol of O_2 , and 5.5 mol of C in the oxy-thermal carbide furnace.

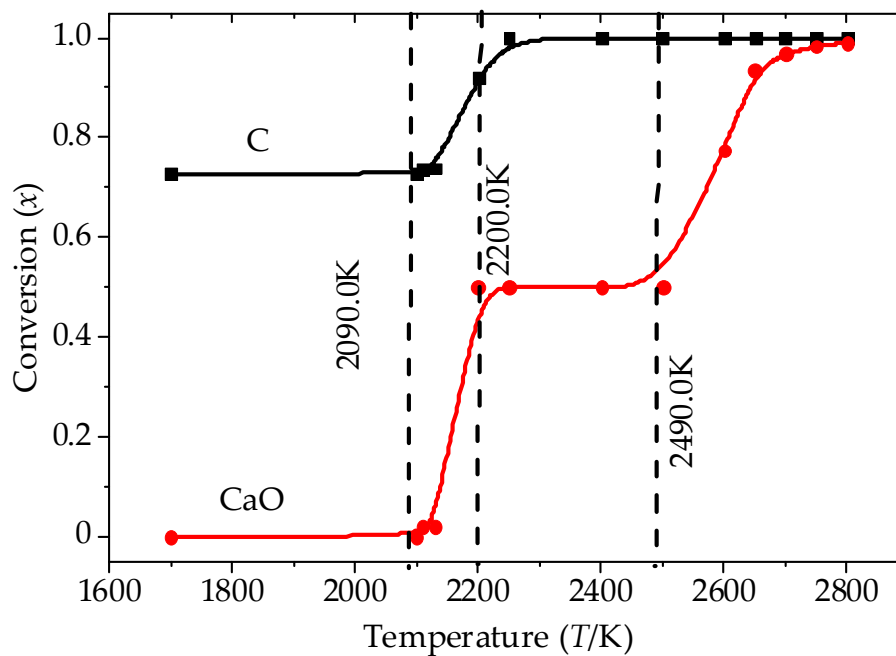


Figure 16. The conversion of C and CaO at each reaction temperature.

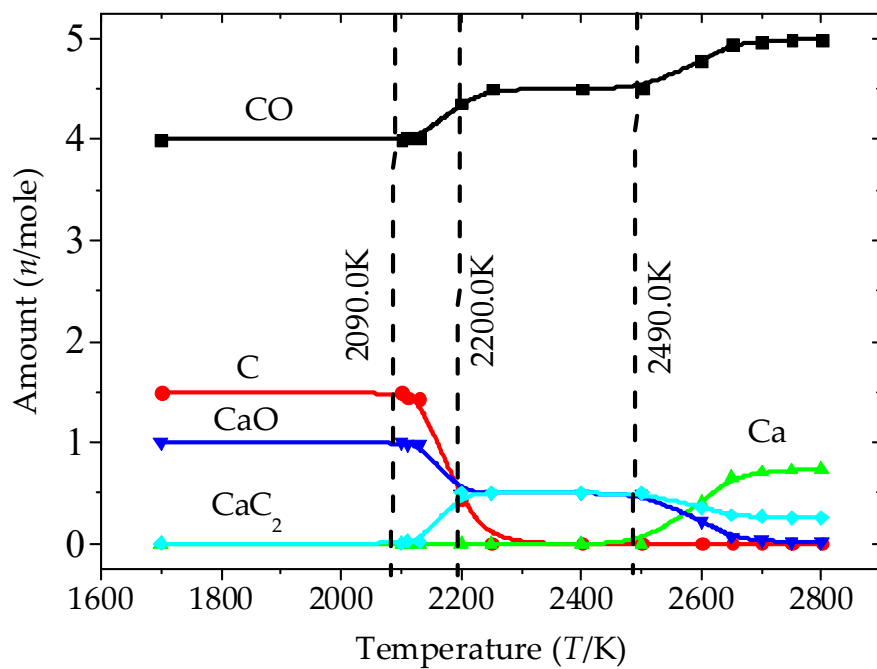


Figure 17. The equilibrium composition at each reaction temperature.

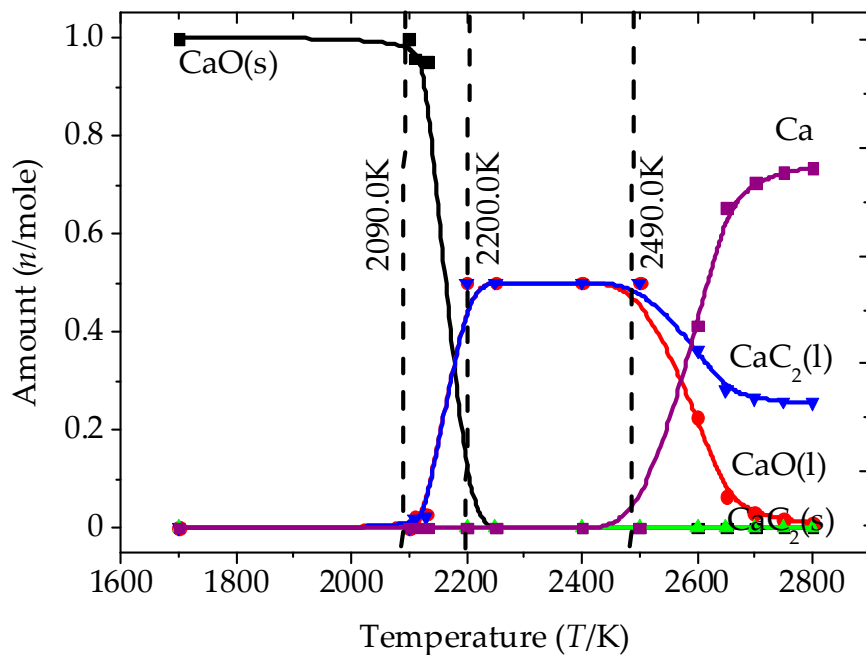


Figure 18. The equilibrium phase composition at each reaction temperature.

Figures 16 and 17 show that, at approximately 2100 K, CaO starts to react with C to produce CaC₂. CaO and C gradually decrease, whereas the conversion of CaO and C increases. CaC₂ reaches a maximum at approximately 2200 K. After 2290 K, the C is completely consumed, but CO, CaC₂ and CaO remain the same. After approximately 2490 K, CaO gradually diminishes, and Ca is rapidly produced. Then, the conversion of CaO is further enhanced to 100% at 2800 K.

Figure 18 shows the chemical reaction equilibrium behavior of the gas–liquid–solid heterogeneous phases under the limited C condition in the oxy-thermal carbide furnace. With the increase of temperature, CaO (s) begins at its maximum, with an initial concentration of 1 mol. When the reaction occurs, CaO (s) quickly melts and decreases to zero, whereas CaO (L) and CaC₂ (L) increase. At

approximately 2200 K, CaO (L) and CaC₂ (L) are nearly identical, with approximate maximums of 0.5 mol and then remain the same afterward. This is because the mole fraction of CaC₂ in the system is within the liquid region in Figure 2. At 2490 K, CaO (L) and CaC₂ (L) decrease gradually, but Ca increases rapidly due to R5 shifting to the formation of products at this temperature, producing a large amount of Ca.

Figures 12–18 illustrate that the maximum conversion of CaO to CaC₂ is 50% in the limited C condition. After 2490 K, R5 occurs, which means that CaC₂ is consumed to react with CaO to produce Ca. Therefore, the excess C condition should be adopted in the practical manufacture of CaC₂. For example, at the condition of excess C and approximately 2370 K, CaC₂ (L) increases and CaO (s) decreases rapidly with temperature. Meanwhile, the conversions of CaO and C reach 90%. This may be considered as a set of appropriate operating conditions.

4. Conclusions

This study demonstrates that the CaC₂ formation mechanism depends on two factors, the amount of C and the CO partial pressure. When the C is in excess and the CO partial pressure is high, the production of Ca is limited; thus, the CaC₂ formation is believed to be a one-step mechanism. However, when there is limited C and the CO partial pressure is low, the production of Ca is promoted; thus, CaC₂ formation is believed to be a two-step mechanism.

The chemical reaction equilibrium behaviors of gas–liquid–solid heterogeneous phases in an oxy-thermal carbide furnace were analyzed at conditions of an excess of C and limited C. At 100 kPa, the equilibrium compositions in the furnace were calculated at different temperature conditions, and approximately 2370 K and 100 kPa is an appropriate condition for the formation of CaC₂. Under these conditions, the conversions of both CaO and C can reach 90%.

Author Contributions: W.X., D.Z., X.C., and W.H. conceived the study. Q.W. analyzed data and made figures. M.G. and Y.M. provided resources for this work. W.X. wrote the paper and all authors contributed to the editing of the manuscript. All authors have read and agreed to the published version of the manuscript.

Funding: This research received no external funding.

Acknowledgments: This work was supported by the National Basic Research Program of China (2011CB201306), the GDAS Special Project of Science and Technology Development (Grant No. 2018GDASCX-0802), and the National Natural Science Foundation of China (51706146). Wenjie Xiong wishes to acknowledge the support from Beijing University of Chemical Technology, Beijing 100029, China, for obtaining his Master's degree in 2015.

Conflicts of Interest: The authors declare no conflict of interest.

References

1. Szmant, H. *Organic Building Blocks of the Chemical Industry*; John Wiley & Sons. Inc.: Hoboken, NJ, USA, 1989; pp. 255–256.
2. Sun, W. Reviews of the calcium carbide industry in 2012 and prospect in 2013. *Econ. Anal. China's Pet. Chem. Ind.* **2013**, *4*, 29–31.
3. Erasmus, L. The application of plasma-arc technology for the production of calcium carbide. In Proceedings of the Electric Furnace Conference Proceedings, Toronto, ON, Canada, 12–15 November 1991; pp. 293–298.
4. Guo, J.; Zheng, D.X. Thermodynamic analysis of low-rank-coal-based oxygen-thermal acetylene manufacturing process system. *Ind. Eng. Chem. Res.* **2012**, *51*, 13414–13422. [[CrossRef](#)]
5. Mi, Y.; Zheng, D.X.; Guo, J.; Chen, X.H.; Jin, P. Assessment of energy use and carbon footprint for low-rank coal-based oxygen-thermal and electro-thermal calcium carbide. *Fuel Process. Technol.* **2014**, *119*, 305–315. [[CrossRef](#)]
6. Tagawa, H.; Sugawara, H. The kinetics of the formation of calcium carbide in a solid-solid reaction. *J. Ceram. Chem. Jpn.* **1962**, *35*, 1276–1279. [[CrossRef](#)]
7. Muller, M. Structure, properties and reactions of CaO in burnt lime. Part 3. Composite reactions of CaO and C in solid and liquid state. *Scand. J. Metall.* **1990**, *19*, 210–217.

8. EI-Nass, M.; Munz, R. Production of calcium carbide in a plasma-jet fluid bed reactor. In Proceedings of the ISPC-12, Minneapolis, MN, USA, 21–25 August 1995; pp. 613–618.
9. EI-Nass, M.; Munz, R.; Ajersch, F. Solid-phase synthesis of calcium carbide in a plasma reactor. *Plasma Chem. Plasma Process.* **1998**, *18*, 409–427. [[CrossRef](#)]
10. Rai, H.; Gregory, N. The time dependence of effusion cell steady-state pressure of carbon monoxide and calcium vapors generated by the interaction of calcium oxide and graphite. *J. Phys. Chem.* **1970**, *74*, 529–534. [[CrossRef](#)]
11. Brookes, C.; Gall, E.; Hudgins, R. A model for the formation of calcium carbide in solid pellets. *Can. J. Chem. Eng.* **1975**, *53*, 527–533. [[CrossRef](#)]
12. Wiik, K.; Raaness, O.; Olsen, S. Formation of calcium from calcium vapor and carbon. *Scand. J. Metall.* **1983**, *13*, 1347–1354.
13. Kim, S.; Raymond, F.; Baddour, B. CaC₂ Production from CaO and coal or hydrocarbons in a rotating-arc reactor. *Ind. Eng. Chem. Process Des. Dev.* **1979**, *18*, 323–328. [[CrossRef](#)]
14. Wang, J.; Kayoko, M.; Takayuki, T. High-temperature interactions between coal char and mixtures of calcium oxide, quartz and kaolinite. *Energy Fuels* **2001**, *15*, 1145–1152. [[CrossRef](#)]
15. Thoburn, W.; Pidgeon, L. Differential thermal analysis of calcium carbide formation. *Can. Metall. Q.* **1965**, *4*, 205–217. [[CrossRef](#)]
16. Li, G.D.; Liu, Q.Y.; Liu, Z.Y. Production of calcium carbide from fine biochars. *Angew. Chem. Int. Ed.* **2010**, *49*, 8480–8483. [[CrossRef](#)] [[PubMed](#)]
17. Muftah, H. Synthesis of Calcium Carbide in a Plasma Spout Fluid Bed. Ph.D. Thesis, McGill University, Montréal, QC, Canada, 1996.
18. Guo, J.; Zheng, D.X.; Chen, X.H.; Mi, Y.; Liu, Z.Y. Chemical reaction equilibrium behaviors of an oxy-thermal carbide furnace reaction system. *Ind. Eng. Chem. Res.* **2013**, *52*, 17773–17780. [[CrossRef](#)]
19. Stals, J.; Peters, C.; Diepen, G. Measurements and calculation of the three-phase equilibrium (solid compound + liquid + gas) in the binary (sulfur dioxide + p-toluidine) where the compound in liquid and gas is dissociated into its components. *J. Chem. Thermodyn.* **1979**, *11*, 1107–1112. [[CrossRef](#)]
20. Ruff, O.; Foerster, E. Calcium carbide, its formation and decomposition. *Z. Anorg. Allg. Chem.* **1923**, *131*, 321–347. [[CrossRef](#)]
21. Flusin, G.; Aall, C. Sur l'étude du système CaC₂-CaO. *Compt. Rend.* **1935**, *201*, 451–453.
22. Li, G.D.; Liu, Q.Y.; Liu, Z.Y. Kinetic behaviors of CaC₂ production from coke and CaO. *Ind. Eng. Chem. Res.* **2013**, *53*, 527–535. [[CrossRef](#)]
23. Kameyama, N. *Electrochemistry: Theory and Applications, Vol. III-2*; Maruzen: Tokyo, Japan, 1956; pp. 134–141.
24. Juza, R.; Schuster, H. The phase diagram of the calcium oxide-calcium carbide system. *Z. Anorg. Allg. Chem.* **1961**, *311*, 62–75. [[CrossRef](#)]
25. Ji, L.M.; Liu, Q.Y.; Liu, Z.Y. Thermodynamic analysis of calcium carbide production. *Ind. Eng. Chem. Res.* **2014**, *53*, 2537–2543. [[CrossRef](#)]
26. Li, G.D.; Liu, Q.Y.; Liu, Z.Y. CaC₂ production from pulverized coke and CaO at low temperature – influence of minerals in coal-derived coke. *Ind. Eng. Chem. Res.* **2011**, *51*, 10748–10754. [[CrossRef](#)]
27. Smith, J.M.; Van Ness, H.C.; Abbott, M.M. *Introduction to Chemical Engineering Thermodynamics*, 6th ed.; McGraw-Hill Co. Inc.: New York, NY, USA, 2001; pp. 390–476.
28. Peng, D.Y.; Robinson, D.B. A new two-constant equation of state. *Ind. Eng. Chem. Fundam.* **1976**, *15*, 59–64. [[CrossRef](#)]
29. Aspen Plus. *Aspen Plus IGCC Mode*; Aspen Technology: Bedford, MA, USA, 2008.
30. Binnewies, M.; Milke, E. *Thermodynamical Data of Elements and Compounds*; Wiley-Vch Verlag GmbH: Weinheim, Germany, 2002.
31. Barin, I. *Thermochemical Data of Pure Substances*, 3rd ed.; Wiley-Vch Verlag GmbH: Weinheim, Germany, 1995; pp. 422–441.
32. Healy, G. The Calculation of an internal energy balance in the smelting of Calcium Carbide. *J. S. Afr. Inst. Min. Metall.* **1995**, *9*, 225–232.
33. Lindberg, D.; Chartrand, P. Thermodynamic evaluation and optimization of the (Ca + C + O + S) system. *J. Chem. Thermodyn.* **2009**, *41*, 1111–1124. [[CrossRef](#)]

34. Vonka, P.; Leitner, J. Calculation of chemical equilibrium in complex system: System restrictions. *Collect. Czech. Chem. Commun.* **2000**, *65*, 1443–1452. [[CrossRef](#)]
35. Aljarrha, M.; Medraj, M. Thermodynamic assessment of the phase equilibria in the Al-Ca-Sr system using the modified quasichemical model. *J. Chem. Thermodyn.* **2008**, *40*, 724–734. [[CrossRef](#)]

Sample Availability: Samples of the compounds are available from the authors.



© 2020 by the authors. Licensee MDPI, Basel, Switzerland. This article is an open access article distributed under the terms and conditions of the Creative Commons Attribution (CC BY) license (<http://creativecommons.org/licenses/by/4.0/>).